

N 66-80830

(ACCESSION NUMBER)

34

(PAGES)

(NASA CR OR TMX OR AD NUMBER)

(THRU)

None

(CODE)

(CATEGORY)

4

COMPARISON OF DETAILED NUMERICAL SOLUTIONS WITH SIMPLIFIED
THEORIES FOR THE CHARACTERISTICS OF THE
CONSTRICTED-ARC PLASMA GENERATOR

Velvin R. Watson*

ABSTRACT

A number of analytical and semianalytical methods for calculating the performance of the constricted-arc plasma generator have been reported. The theoretical models for these methods contain rough approximations for obtaining the analytical or semianalytical solutions. Recently, numerical methods have been applied to obtain the performance of a more complete model with fewer approximations. Since the analytical solutions of simplified models are valuable for obtaining scaling laws or for gaining insight into the arc column behavior, it is important to determine the effect of the rough approximations upon the accuracy of the solutions. This paper illustrates the effect of these approximations on the accuracy of the analytical solutions by comparing the approximate solutions from the several simplified models with the more complete numerical solutions. It is demonstrated that none of the simplified models is capable of presenting a realistic physical picture.

Special emphasis is given to the comparison of the numerical solutions with the analytical solutions of the Stine-Watson model. It is shown that this model does not present a reasonable picture of the enthalpy distribution, nor is the assumed mass flux distribution realistic. However, this model does present a fair picture of the energy flux distribution, electrical characteristics, and wall heat flux for constricted-arc plasma generators with the gases, air and nitrogen, and for constrictor diameters and pressures where radiation heat losses are negligible compared to thermal conduction losses.

The Eckert and Anderson model that considers transpiration wall cooling is shown to predict overly optimistic enthalpies. The numerical calculations show that, with nitrogen and hydrogen gases, water-cooled constrictors yield higher enthalpies than transpiration-cooled constrictors.

The Chen and Weber semianalytical models which divide the gas into a core flow and outer flow do not present a realistic physical picture of the energy flux distribution, but do present a fairly accurate picture of the enthalpy distribution.

Based on the comparisons presented, the more simplified models are considered satisfactory only for limited scaling or for very rough estimates for preliminary design studies, and the numerical calculations, which at present require approximately 2 minutes computing time, are recommended for more accurate performance studies or for final design criteria.

*Research Scientist, National Aeronautics and Space Administration, Ames Research Center, Moffett Field, California.

INTRODUCTION

The constricted thermal arc is employed for the production of very hot, dense plasma flows, for the production of the very high heat fluxes required in material testing, for the experimental measurement of transport properties, and for propulsion. A number of theoretical models for predicting the performance of this constricted thermal arc have been reported, and these models have been very useful. For example, the simplified theoretical model formulated by Stine and Watson⁽¹⁾ gave sufficient insight into the arc behavior to allow development of the high-performance plasma generator shown in Fig. 1.

None of the models proposed thus far, however, are exact in that none display an accurate physical picture of all the important features of the arc column. The shortcomings result from the rough approximations and assumptions required for obtaining an analytical or semianalytical solution for each model. Therefore, in order to make intelligent use of these simplified models, one must know which of the arc column characteristics each model represents properly, and which of the characteristics are poorly represented.

Until recently, there were no satisfactory methods for determining the accuracy with which these simplified theoretical models represent the arc column. The assumptions common to all models are that the gas flow is laminar and the arc is steady. Recent experiments by Shepard⁽²⁾ have, however, demonstrated that indeed the flow is laminar and the arc is steady.

Additional assumptions are introduced into each of the theoretical models to approximate the distribution of mass flux within the constrictor. Several gas thermodynamic and transport properties are also linearized in the Stine-Watson model. The accuracy of the models and the approximations entering into their formulation can now be evaluated with a numerical program⁽³⁾ that solves for the properties of the constricted arc with axial gas flow. Within this program the distribution of mass flux, rather than being assumed a priori, is determined by the simultaneous solution of the momentum, continuity, and energy equations; and theoretical gas properties for real equilibrium gas are introduced rather than linearized gas properties. The solutions from this numerical program give the arc column characteristics in considerable detail and, therefore, can be used effectively to evaluate the simplified models.

The purpose of this paper is to compare the numerical solutions with each of the simplified theoretical models in order to determine which of the characteristics the simplified model displays properly, and which it represents poorly.

THE SIGNIFICANT CHARACTERISTIC FEATURES OF THE CONSTRICTED THERMAL ARC

In order to evaluate the simplified models, one must first understand the characteristic features of the constricted thermal arc. Therefore, the outstanding features suggested by the numerical calculations are discussed in what follows.

The distributions of energy, mass flux, energy flux, velocity, and momentum flux within the constricted thermal arc that result from the numerical calculations are illustrated by means of three-dimensional plots such as the graph in Fig. 2. This figure illustrates the spatial enthalpy distribution within a

constrictor of 1.27-cm diameter. The arc is assumed to be symmetrical about the constrictor axis, and all properties are functions only of radial and axial position. The radial position is shown on the horizontal axis; the axial position is shown on the oblique axis; and the arc properties (in this case enthalpy) are shown on the vertical axis.

There are three important characteristic features to note in this figure. First, the enthalpy tends to "overshoot," reaching a maximum near the entrance of the constrictor. Second, the enthalpy profile within the hot core rapidly approaches a nearly constant shape, such that there is only a small change in the radial profile downstream of the entrance region. Third, although the core enthalpy profile quickly approaches a constant shape, the core spreads to the constrictor wall relatively slowly.

The remaining property distributions are illustrated in Fig. 3. From the graph of mass flux, one can see that most of the flow is forced to the wall at the constrictor entrance, and as the gas proceeds downstream, it is slowly ingested into the core of the arc. Although the radial profiles of enthalpy and mass flux vary radically with axial distance, the energy flux profiles remain nearly similar for all axial positions, with the magnitudes of the profiles increasing near the constrictor inlet and approaching an asymptotic value downstream. The radial velocity profiles are approximately parabolic, similar to Poiseuille flow, except that within the constricted arc the velocity gradients are caused mainly by large density gradients rather than by viscous forces. The graph of momentum flux illustrates that near the constrictor inlet, momentum is convected to the constrictor walls causing the "ears" on the momentum flux profiles near the constrictor inlet. Farther downstream, as the gas is ingested into the arc core, the momentum is convected radially inward, causing high momentum flux in the center of the arc. The ears downstream appear to be caused by large variations in gas viscosity since they disappear when the viscosity is set equal to zero.

From the local arc properties discussed above, one can obtain other arc column characteristics of interest. Several of the more interesting are illustrated in Fig. 4. Of particular interest is the mass average enthalpy because it is a measure of the total energy in the gas. The mass average enthalpy increases near the constrictor inlet, and approaches an asymptotic value downstream. In the asymptotic region, the heat added to the gas from ohmic heating is exactly balanced by the heat loss to the constrictor wall.

Also important are distributions with length of voltage gradient, wall heat-transfer rate, and static pressure. The voltage gradient is nearly uniform over the length of the constrictor except near the constrictor inlet where it becomes very high. The heat-transfer rate is low near the inlet and increases to a maximum value at the exit. That portion of heat-transfer rate due to conduction is very low until the enthalpy profile spreads to the constrictor wall. The pressure decreases nearly linearly over most of the constrictor, but decreases most rapidly near the exit where the flow is aerodynamically choked. At choking the static pressure is approximately one-half the pressure at the constrictor inlet.

For the constricted arc discussed above, the radiation heat loss was approximately one-half of the total. Whenever radiation becomes the dominant heat-loss mechanism, the arc column characteristics are modified as shown in Figs. 5 and 6. The most striking difference caused by radiation is the flattened enthalpy profiles shown in Fig. 5. The flat profiles also imply a considerable decrease in the enthalpy of the gas that can be contained in any given constrictor. Furthermore, the wall heat flux shown in Fig. 6 is no longer a maximum at the constrictor exit. Rather, it is a maximum at the constrictor inlet where the pressure is the highest.

COMPARISON OF THE SIMPLIFIED THEORETICAL
MODELS WITH THE NUMERICAL SOLUTIONS

None of the simplified theoretical models which have been proposed to represent the constricted thermal arc display all of the important phenomena discussed above. Nevertheless, each represents a few of the more important arc column characteristics fairly well. These models can be used to advantage if one is familiar with which of the characteristics each predicts reasonably, and which of the characteristics are not represented properly. The following comparison of the theoretical models with the numerical calculations brings to light the relative ability of each model to display the important arc column phenomena.

Stine-Watson Model

The first model to be compared to the numerical calculations, the Stine-Watson model,⁽¹⁾ is the simplest and requires the greatest number of rough approximations; in fact, sufficient approximations were made to obtain a completely analytical solution. This is the only model representing the entire arc, from the constrictor entrance to the constrictor exit, for which the solutions are analytical. The approximations inherent in this model will be discussed in more detail after the model is compared with the numerical calculations so that the validity of the approximations and their effect on the solution can be evaluated.

Figure 7 compares the enthalpy, mass flux, and energy flux of the Stine-Watson model with the numerical solution. Neither the enthalpy distribution nor the mass flux distribution is represented reasonably. In particular, the model does not display the enthalpy "overshoot," the rapid approach of the core enthalpy profile to a constant shape, nor the slow spread of the core to the constrictor wall. The mass flux distribution does not display the spreading of the gas to the wall near the inlet nor the gradual return of the gas to the arc core, but the mass flux distribution at the constrictor exit is represented approximately. Finally, the energy flux distribution is represented fairly well by the model.

The remaining important characteristics are shown in Fig. 8. One can see that the center-line enthalpy is not represented properly by the model, the trends of the space average enthalpy and the wall heat flux are represented crudely, and the trends of the mass average enthalpy and voltage gradient are represented fairly well. The model does not yield the change of gas pressure with length.

The approximations incorporated in this model can now be examined. The complete list of the approximations is given and discussed in Ref. 1, and only those found to be most crude will be investigated here. They are as follows:

1. The mass flux is assumed to be constant throughout the constrictor.
2. The enthalpy profile at the constrictor inlet is taken to be the zeroth order Bessel function of the first kind because this is the only starting profile for which an analytical solution for the model can be obtained.
3. The radiation heat loss is neglected.
4. The remaining gas properties of major importance - thermal conductivity potential, and electrical conductivity - are assumed to be linearly related to enthalpy.

As was shown previously in Fig. 7, the assumption of constant mass flux throughout the constrictor is very poor, especially near the constrictor inlet. However, the mass flux does tend to become more uniform downstream, and for moderate characteristic lengths (z/z_0 greater than 0.1), is nearly uniform across the constrictor.

The remaining approximations can best be evaluated by incorporating each one in the numerical solutions and observing whether the solutions change appreciably. A radical change would indicate that the approximation was a poor one.

The graphs on the left of Fig. 9 show the numerical solution in which the starting enthalpy profile is a Bessel function. For comparison, the graphs on the right are for what is thought to be a more probable starting enthalpy profile. Although there is some difference between the two cases near the constrictor inlet, this difference rapidly disappears downstream. Therefore, this approximation, although probably not realistic, does not seriously affect the solution, particularly the solution near the constrictor exit.

Figures 10 and 11 illustrate the effect of neglecting the radiation heat loss, which accounts for approximately half the total loss from the arc column illustrated on the right. The enthalpy profiles are flattened by the radiation loss, but the mass flux and energy flux distributions are not severely changed. The comparisons in Fig. 11 show that the major discrepancy between the Stine-Watson model and the complete numerical solutions for the exit mass average enthalpy is due to the approximation that the radiation heat loss is neglected. On the other hand, the wall heat flux of the Stine-Watson model is more representative of the arc with moderate radiation losses than of the arc with no radiation losses. However, when the radiation losses become dominant, the Stine-Watson model will grossly underestimate the wall heat flux. Since the radiation losses increase rapidly with increasing pressure, the Stine-Watson model should not be applied to the 1.27-cm-diameter constrictor at pressures appreciably larger than atmospheric.

The effect of linearizing the relationship between enthalpy, thermal conductivity potential, and electrical conductivity is shown in Fig. 12. This approximation does not cause any major discrepancy from the more complete numerical solution.

From the discussion, it should now be apparent that, although there is satisfactory agreement between the theoretical model and experimental measurements for some of the arc column characteristic,⁽⁴⁾ for example, as shown in Fig. 13, this agreement does not imply a completely correct model. The model is useful for making preliminary estimates of the mass average enthalpy of the gas, the voltage gradient, and the constrictor heat-transfer rate along the constrictor for small constrictors at moderate pressure, but not for estimating mass flux or local enthalpy distributions.

Core Flow Model

The least satisfactory approximation used in the Stine-Watson model is that the mass flux is constant throughout the constrictor. Chen recognized that near the constrictor inlet, the mass flux near the axis of the constrictor would be small, and he proposed the model⁽⁵⁾ shown in Fig. 14. The flow is divided into three regions. The mass flux in the core is assumed to be identically zero. The enthalpy of the core is assumed to be given by the Elenbaas-Heller equation, and is independent of the mass flow. The energy transferred to the gas outside the core is calculated by assuming the core is a solid rod, and equations for forced convection past the solid rod are employed.

This model does give a realistic picture of the mass flux at the constrictor inlet and of the enthalpy distribution. However, the mass flux downstream and the energy flux throughout the constrictor are not shown properly. Furthermore, this model requires numerical calculations of the core properties and iterative matching of the heat transfer from the core with the heat transfer to the inner flow. Therefore, the calculating times required for obtaining predictions from this model are orders of magnitude longer than the calculating times for the Stine-Watson model, and perhaps not much shorter than the computing times for the complete numerical calculations, which take approximately 2 minutes.

Weber Model

Weber recently developed a model⁽⁶⁾ which displays the maximum enthalpy near the constrictor inlet, the slow spread of the core to the constrictor wall, and the ingestion of the cold outer flow into the arc column core. This is the most realistic of the simplified models proposed, but it is also the most complex and requires iterative matching of numerically calculated core properties with the properties of the outer flow. Furthermore, an assumption is required for obtaining the distribution of mass flux; Weber originally chose the assumption such that the average mass flux in the core was the same as the average mass flux of the outer flow. With this assumption, the properties calculated using this model would appear qualitatively as sketched in Fig. 15; the numerical calculations shown previously are also shown for comparison. Here again, the enthalpy distribution is represented fairly well, but the mass flux and energy flux distributions are poorly represented. With a closer approximation for the mass flux (e.g., a closer approximation would result from the assumption that the Mach number is constant on planes perpendicular to the axis of the constrictor), this model should yield a fair representation of the constricted arc.

Weber's model, however, is not a simple analytical model that can be used for quick approximations of the more important arc column characteristics (e.g., the total energy of the gas leaving the constrictor). The computing time for this model is probably of the same order of magnitude as the computing time for the more complete numerical solutions presented at the beginning of this paper. Therefore, rather than use this semianalytical model, it is probably more advantageous to use the more simplified models for rough preliminary approximations and then proceed directly to a more precise numerical solution for more accurate predictions of constricted arc performance.

Eckert-Anderson Model

The last model to be compared with numerical solutions includes transpiration cooling of the constrictor wall⁽⁷⁾ and solves only for the asymptotic enthalpy profile. Solutions were obtained in analytical form for several assumed radial mass flux profiles and with an idealized gas. (The idealized gas is identical to that of the Stine-Watson model, except that a constant value of radiance is included.) The solutions are simple enough to yield the approximate governing parameters for the arc column behavior; therefore, this model should prove helpful. In fact, later comparisons will illustrate that the behavior of the arc within the water-cooled constrictor is very similar to that of the arc within the transpiration-cooled constrictor; so this model may also have some application for predicting the enthalpy of the arc column within the water-cooled constrictor.

Unfortunately, Eckert and Anderson⁽⁷⁾ extrapolated the relationship between the theoretical enthalpy and the thermal conductivity potential⁽⁸⁾ in the linear

manner shown in Fig. 16. This procedure resulted in a low estimate of heat conduction. Also, they selected as radial distributions of mass flux those shown in Fig. 17 rather than a radial distribution similar to the numerically calculated distribution, also shown in Fig. 17, which results in high estimates of heat convection. Therefore, they predicted enthalpies within the constrictor which are an order of magnitude higher than the enthalpies determined by the numerical solutions.

From these predictions, Eckert and Anderson concluded that significantly higher enthalpies could be obtained within transpiration-cooled constrictors than within water-cooled constrictors. The following comparisons indicate that this conclusion may not be correct.

The aerodynamically choked arc column in the transpiration-cooled constrictor with uniform blowing rate is compared to the arc column in the water-cooled constrictor with the same exit mass flow in Figs. 18, 19, and 20. The graphs on the left side of Figs. 18 and 19 are numerical calculations of the arc column in hydrogen within the transpiration-cooled constrictor, and the graphs on the right are numerical calculations for a similar arc column in a water-cooled constrictor. The two major differences between the arc column in the transpiration-cooled constrictor and the arc column in the water-cooled constrictor are, first, that the enthalpy profile in the former approaches an asymptotic value more rapidly than in the latter and second, that the heat transfer to the constrictor wall is considerably less for the former than for the latter. (The ears on the energy flux distributions appear to be caused by dissociation as they occur at the dissociation temperature of hydrogen.)

Although transpiration cooling reduces the heat transfer to the constrictor wall, it does not reduce this heat transfer sufficiently to make the transpiration-cooled constrictor superior to the water-cooled constrictor. The heat flux to the water-cooled constrictor, shown in Fig. 20, is within the capabilities of water cooling, but the lower heat flux to the transpiration-cooled constrictor cannot be entirely absorbed by the flow of the gas through the wall. (The maximum cooling obtainable by the flow of the gas through the wall is also shown in Fig. 20.) Therefore, additional cooling would be required for this transpiration-cooled constrictor in order to maintain the assumed constant wall temperature. From this comparison, there appears to be no major advantage of transpiration cooling over water cooling.

The similarities between the arc column within the transpiration-cooled constrictor and that within the water-cooled constrictor are striking. The arc in the water-cooled constrictor forces the gas to the wall, and the gas then bleeds slowly into the arc core in a manner similar to the process within the transpiration-cooled constrictor.

Applicability of the Models for High Pressure Arcs

All of the above comparisons were made for the constricted arc in which radiation heat losses are not the dominant heat loss mechanism. Unfortunately, none of the simple models can be used for accurately predicting of arc column characteristics when radiation heat losses are dominant because these heat losses depend strongly on pressure, and none of the simplified models yield information on the pressure gradient within the constrictor. Numerical techniques are believed to be the only methods at present that can reasonably predict arc column characteristics at high pressures when radiation losses are dominant, and even these solutions may contain considerable error because of the large errors possible in the theoretical values of gas radiance.

CONCLUSIONS

The preceding comparisons illustrate that none of the simplified models presented yield a picture of the phenomena occurring within the constricted-arc plasma generator that agrees in all respects with the picture emerging from the more complete numerical calculation procedure. Nevertheless, the Stine-Watson model provides a very simple method for obtaining rough estimates of the total energy of the gas at the constrictor exit, the distribution of energy flux throughout the constrictor, the constrictor wall heat flux, and the voltage gradient for the arc column in small constrictors at moderate pressures.

The models which separate the flow into a core flow and outer flows represent some of the arc column phenomena better than the Stine-Watson model, but are still crude. Since these models require the use of a high-speed computer, they do not offer the advantage of yielding quick, rough predictions of arc column behavior. Furthermore, the computing times for the complete numerical calculations presented at the beginning of this paper are not long (approximately 2 minutes). Therefore, the best method for predicting constricted-arc performance appears to be to use the analytical model for establishing the approximate range of interesting constrictor sizes, currents, and flow rates, and to use the complete numerical calculations for obtaining more accurate predictions of constricted-arc performance within this range of interest.

NOMENCLATURE

A = cross-sectional area of the constrictor, m^2

Ag = parameter of the approximation $\sigma = Ag\phi$, mho/watt

c_p = specific heat at constant pressure, J/kg $^{\circ}K$

E = voltage gradient, V/m

E_{∞} = theoretical asymptotic voltage gradient = $2.4/RA_g^{1/2}$, V/m

H_m = mass average enthalpy, J/kg (ref. $H_m = 0$ at $0^{\circ} K$)

H_s = enthalpy averaged over space, J/kg (ref. $H_s = 0$ at $0^{\circ} K$)

H_{∞} = theoretical asymptotic mass average enthalpy = $0.133 c_p I/kRA_g^{1/2}$,
J/kg

h = local enthalpy, J/kg (ref. $h = 0$ at $0^{\circ} K$)

h_c = center-line enthalpy

h_{∞} = theoretical asymptotic center-line enthalpy = $0.307 c_p I/kRA_g^{1/2}$,
J/kg

I = current, amp

k = thermal conductivity, watts/m $^{\circ}K$

\dot{m} = transpiration mass flux

p = pressure, newtons/m²

p_0 = stagnation pressure

q = local heat transfer from the surface of the arc column, watts/m²

q_∞ = theoretical asymptotic wall heat flux = $0.383 I/RA_g^{1/2}$, watts/m²

r = radial distance from the axis of the arc column, m

R = constrictor radius

u = axial velocity, m/sec

v = radial velocity, m/sec

\dot{w} = mass flow rate, kg/sec

z = axial distance along the column, m

z_0 = theoretical characteristic arc column length = $\dot{w}c_p/\pi k$, m

(The arc column properties are nearly asymptotic for $z > 0.1 z_0$.)

ρ = density, kg/m³

σ = conductivity function $\int k \, dT$, watts/m (Ref. $\varphi = 0$ at 0°K)

REFERENCES

1. Stine, H. A., and V. R. Watson, The Theoretical Enthalpy Distribution of Air in Steady Flow Along the Axis of a Direct-Current Arc, NASA TN D-1331, 1962.
2. Shepard, C. E., and V. R. Watson, "Performance of a Constricted-Arc Discharge in a Supersonic Nozzle," Proc. Fifth Biennial Gasdynamics Symposium, Northwestern University Press, 1963.
3. Stine, H. A., V. R. Watson, and C. E. Shepard, "Effect of Axial Flow on the Behavior of the Wall-Constricted Arc," AGARD Specialists' Meeting, Belgium, 1964.
4. Cann, G. L., R. D. Buhler, R. L. Harder, and R. A. Moore, Basic Research on Gas Flows Through Electric Arcs-Hot Gas Containment Limits, Aerospace Research Laboratory, ARL 64-49, 1964.
5. John, R. R., H. Debolt, M. Hermann, W. Hogan, A. Kusko, and R. Liebermann, Theoretical and Experimental Investigation of Arc Plasma-Generation Technology - Part I, ASD-TDR-62-729, September 1963.
6. Weber, H. E., "Constricted Arc Column Growth," Proc. 1964 Heat Transfer and Fluid Mechanics Inst., June 1964.

7. Eckert, E. R. G., and J. E. Anderson, "Performance Characteristics of a Fully Developed Constricted Transpiration-Cooled Arc," AGARD Specialists' Meeting, Belgium, 1964.
8. John, R. R., et al., Theoretical and Experimental Investigation of Arc Plasma-Generation Technology - Part II, ASD-TDR-62-729, September 1963.

FIGURES

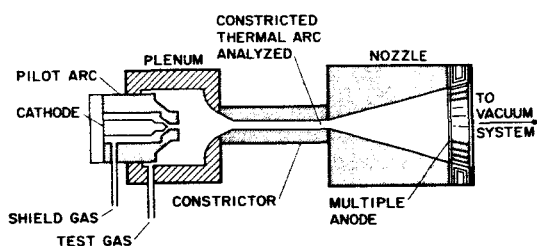


Fig. 1. The Constricted-arc plasma Generator

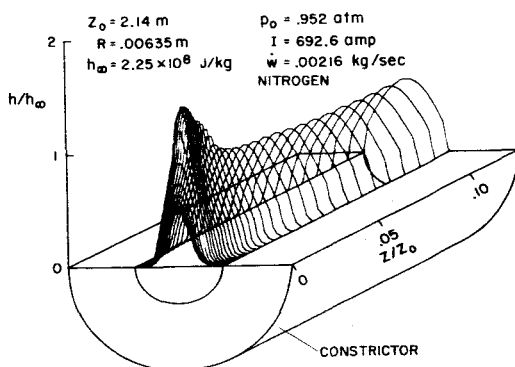


Fig. 2. Distribution of Enthalpy Within the Constricted Arc

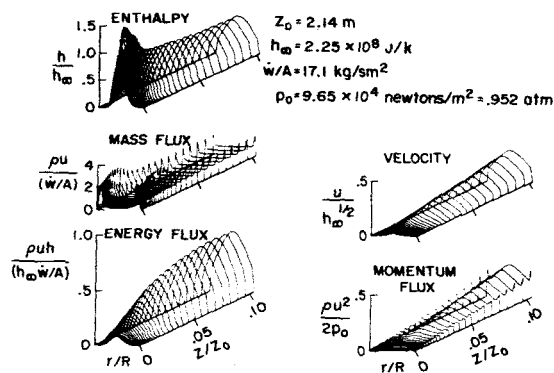


Fig. 3. Characteristic Properties of the Constricted Arc - Spatial Distributions.
($I = 692.6$ amps, $\dot{w} = 0.00216$ kg/s,
 $R = 0.00635$ m)

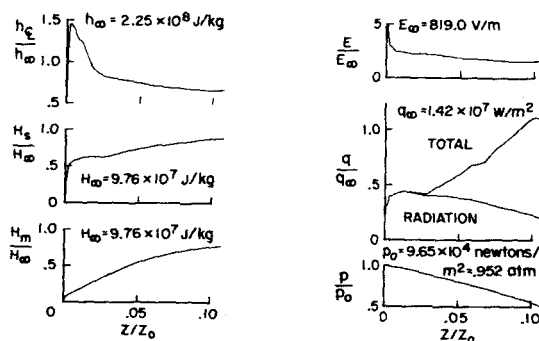


Fig. 4. Characteristic Properties of the Constricted Arc - Axial Distributions.
($I = 692.6$ amps, $\dot{w} = 0.00216$ kg/s,
 $R = 0.00635$ m, $z_0 = 2.14$ m)

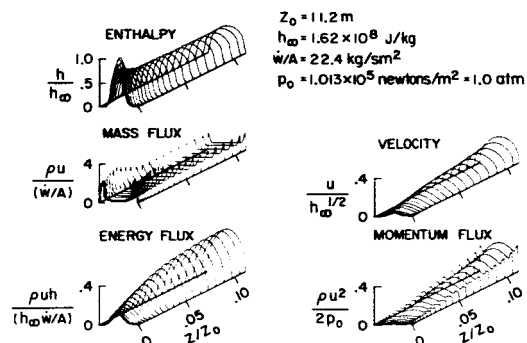


Fig. 5. Characteristic Properties of the Constricted Arc with Large Radiation Heat Losses - Spatial Distributions.
 (I = 1000 amps, $\dot{w} = 0.0113$ kg/s, R = 0.0127 m)

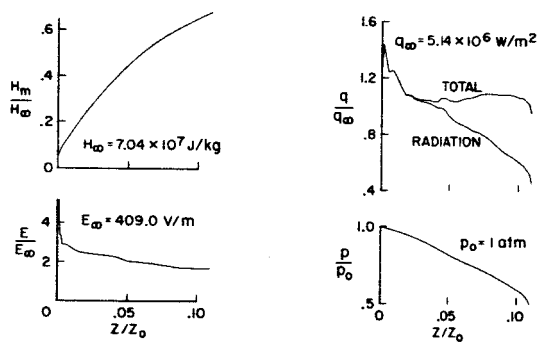


Fig. 6. Characteristic Properties of the Constricted Arc with Large Radiation Heat Losses - Axial Distributions.
 (I = 1000 amps, $\dot{w} = 0.0113$ kg/s, R = 0.0127 m, $z_0 = 11.2 \text{ m}$)

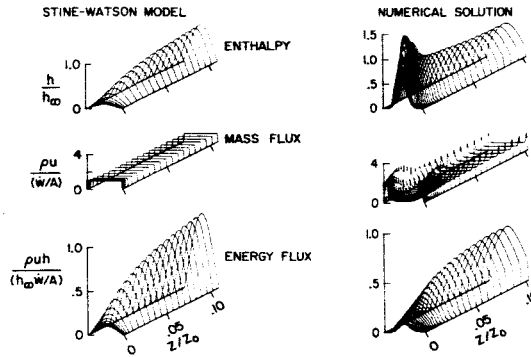


Fig. 7. Comparison of the Stine-Watson Model with Numerical Solutions - Spatial Distributions

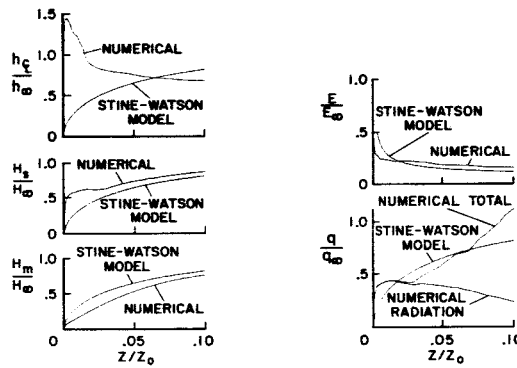


Fig. 8. Comparison of the Stine-Watson Model with Numerical Solutions - Axial Distributions

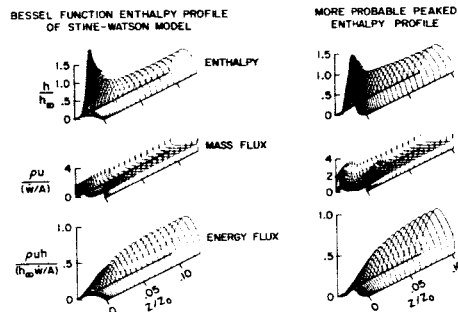


Fig. 9. Effect of Starting Enthalpy Profile on the Solutions for the Constricted Arc

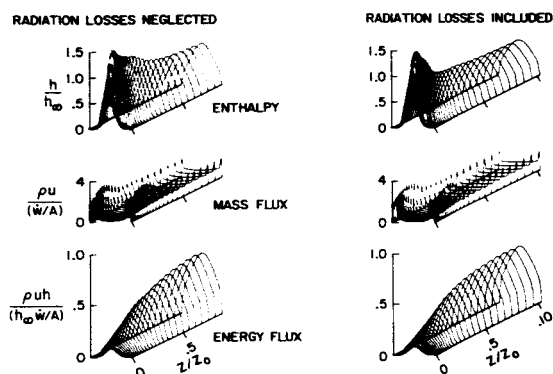


Fig. 10. Effect of Neglecting Radiation Heat Losses - Spacial Distributions

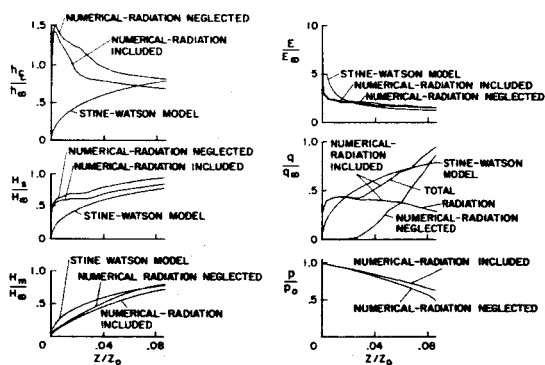


Fig. 11. Effect of Neglecting Radiation Heat Losses - Axial Distributions

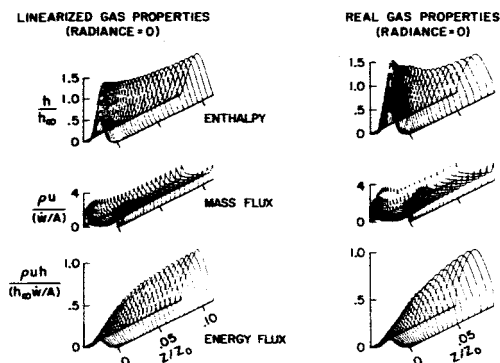


Fig. 12. Effect of Linearizing the Gas Property Relationships

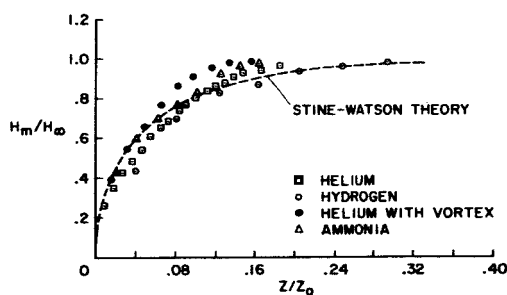


Fig. 13. Comparison of Various Experimental Data to the Stine-Watson Model (from Ref. 4)

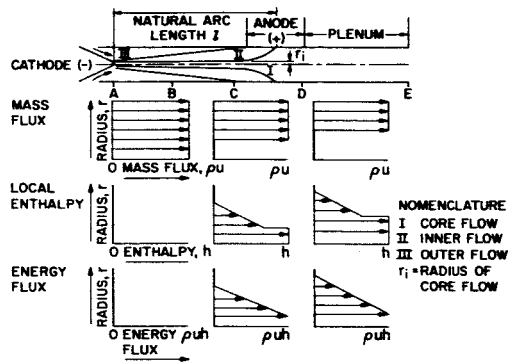


Fig. 14. Core Flow Model Proposed by Dr. Chen
(From Ref. 5)

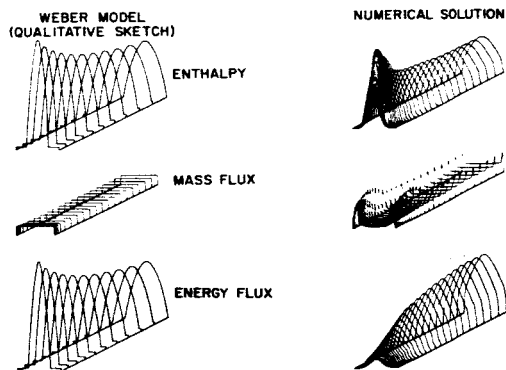


Fig. 15. Core Flow Model Proposed by Dr. Weber

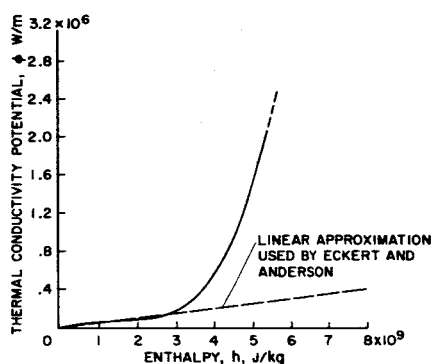


Fig. 16. Linearization of Hydrogen Properties Used by Eckert and Anderson (Hydrogen Properties from Ref. 8)

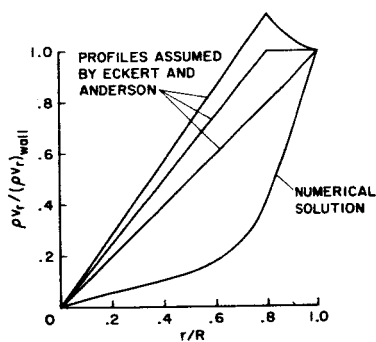


Fig. 17. Assumed Radial Mass Flux for Eckert and Anderson Model

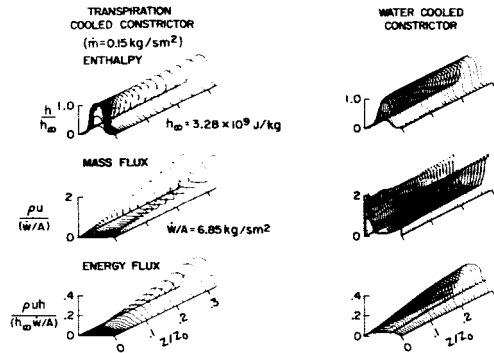


Fig. 18. Comparison of the Arc Columns within Transpiration-cooled and Water-cooled Constrictors - Spatial Distributions. ($I = 1000$ amps, exit $\dot{w} = 5.38 \times 10^{-2}$ kg/s, $R = 0.005$ m, $z_0 = 3.42$ m)

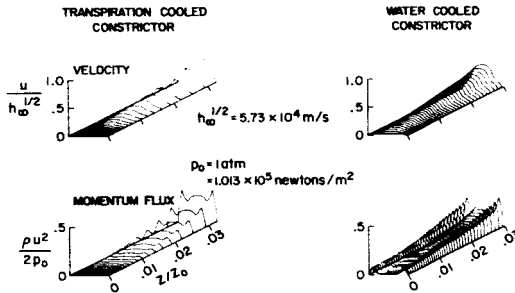


Fig. 19. Comparison of the Arc Columns within Transpiration-cooled and Water-cooled Constrictors - Spatial Distributions. ($I = 1000$ amps, exit $\dot{w} = 5.38 \times 10^{-2}$ kg/s, $R = 0.005$ m, $z_0 = 3.42$ m)

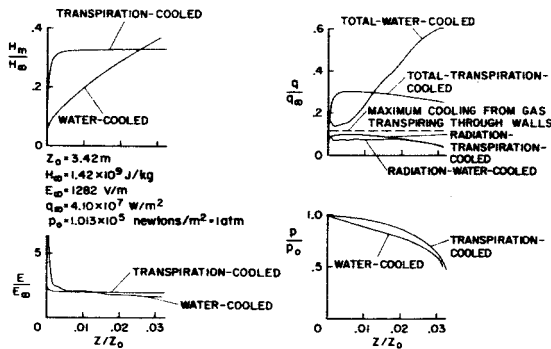


Fig. 20. Comparison of the Arc Columns within Transpiration-cooled and Water-cooled Constrictors - Axial Distributions. ($I = 1000$ amps, exit $\dot{w} = 5.38 \times 10^{-2}$ kg/s, $R = 0.005$ m, $z_0 = 3.42$ m)